Applied Mathematical Modelling 39 (2015) 934–946

Contents lists available at ScienceDirect

Applied Mathematical Modelling

journal homepage: www.elsevier.com/locate/apm

Size-dependent dynamic pull-in analysis of beam-type MEMS under mechanical shock based on the modified couple stress theory

Amir R. Askari, Masoud Tahani *

Department of Mechanical Engineering, Ferdowsi University of Mashhad, Mashhad, Iran

ARTICLE INFO

Article history:
Received 11 May 2013
Received in revised form 20 November 2013
Accepted 12 July 2014
Available online 25 July 2014

Keywords:
MEMS
Mechanical shock
Electrostatic actuation
Modified couple stress theory

ABSTRACT

Size-dependent stability analysis of a fully clamped micro-electro-mechanical beam under the effect of shock acceleration pulse is the objective of present paper. The size-dependent Euler–Bernoulli beam model based on the modified couple stress theory (MCST) with von Kármán-type geometric non-linearity is utilized in theoretical formulations. The non-linear governing differential equation of motion is derived using Hamilton's principle and solved using a simple and computationally efficient single degree-of-freedom (SDOF) approach. The model's predictions based on the classical theory (CT) are compared with those obtained using the finite element method (FEM) and six modes Galerkin approximations in previous studies and an excellent agreement between them is achieved. It is shown that the present SDOF predictions agree better with the FE results than those obtained using six modes approximations for high shock accelerations. Furthermore, the present model can remove the limitation of previous models in capturing dynamic pull-in instability under enormous shock accelerations. A parametric study is also conducted to show the significant effects of couple stress components on micro-beam motion. It is found that the size effect on both dynamic pull-in voltage and maximum amplitude of micro-beam oscillations is usually negligible, when the ratio of beam thickness to the material length scale parameter is larger than 15.

1. Introduction

Micro-electro-mechanical systems (MEMS) are mostly used as sensors and actuators. Because of their small size, low power consumption and the reliability of batch fabrications, there are lots of potential applications in engineering. Clamped–clamped micro-beams represent major structural components and play crucial roles in these systems. One of the most important phenomena associated with electrostatically-actuated MEMS is pull-in instability which is occurred when input voltage exceeds its critical value. In this manner the non-linear electrostatic force will overcome the elastic restoring force, so the movable part is suddenly collapsed toward the substrate. Nathanson et al. [1] and Taylor [2] observed pull-in phenomenon experimentally. If the rate of applied voltage is not negligible, the effect of inertia should be taken into account for pull-in voltage. This type of instability is called dynamic pull-in instability.

* Corresponding author. Tel.: +98 513 8806055; fax: +98 513 8763304.
E-mail address: mtahani@um.ac.ir (M. Tahani).

http://dx.doi.org/10.1016/j.apm.2014.07.019
0307-904X/

Mechanical shock can induce highly dynamic loads on structures causing several types of fracture problems. In MEMS, shock loads can cause micro-structures to hit the stationary electrodes underneath them and causing some undesirable problems such as stiction [3], short circuits [4] and hence failure in the device's function. The majority of micro-structures are fabricated of silicon or polysilicon which are very tough against bending stresses induced from shock acceleration, so failure in MEMS unlike failure in large scale devices does not due to high stresses [5]. The most important source of failure in MEMS is stiction and electric short circuits; however the incidents between a movable part and other parts or a substrate may lead to failure due to the severe contact stresses.

A shock can be defined as a force applied suddenly over a short period of time relative to natural period of structure [6]. A shock load can be characterized by its maximum value, duration and shape. The shock pulse shape in most of cases can be considered as half-sine [6–8]. The response of micro-structures to shock loads has been studied by many researchers. Béliveau et al. [9] characterized experimentally the response of commercial accelerometers due to shock loads and observed some unexpected responses. Brown et al. [10] investigated commercial accelerometers and a pressure sensor to high-g tests. They reported peculiar modes of failure under severe shock conditions and concluded that improved dynamic modeling and characterization of MEM devices under shock load are needed. Fan and Shaw [11] simulated the response of a comb-drive accelerometer subjected to severe dynamic shock loads in all directions. They developed a finite element (FE) model using the software ABAQUS with full non-linear and contact stress capability and remarked that this problem requires a highly non-linear transient dynamic analysis, which is computationally very expensive. Some authors used equivalent lumped spring-mass model to approximate the dynamic response of micro-structures. Their point of view was proper for rough estimation and could not provide an accurate analysis. For example, Li and Shemansky [12] studied the motion of MEM accelerometers during the drop tests. They used both of SDOF and distributed-parameter model to calculate maximum deflection of cantilever and hinged-hinged beam. Some researchers analyzed micro-structures based on distributed-parameter models. Fang et al. [5] investigated the response of a micro-cantilever to a half-sine shock pulse using beam model. They utilized the assumed modes method to calculate displacement and bending stresses of the micro-beam. It is noted that most of the authors investigated the effect of shock pulse lonely and they did not account for the interaction between electrostatic excitation and shock pulse acceleration effect. Younis et al. [13] accounted for the dynamic interaction between these excitations. They used both SDOF and beam model to investigate the response of micro-beam under combined effect of these two excitations. They used the Galerkin based reduced order (six modes approximations) model to solve the governing equation of the beam. Younis et al. [14] also analyzed the response of mechanical shock on micro-structures incorporating the effect of packaging. They used six modes approximation in the Galerkin-based reduced order model to simulate the response of micro-structure to the combination of shock acceleration and electrostatic excitation. They verified their model by comparing its results with those prepared utilizing commercial finite element software ANSYS. It was shown that the combination of a shock load and an electrostatic actuation makes the instability threshold much lower than the threshold predicted, considering the effect of shock alone or electrostatic actuation alone [13,14]. It should be noted that neither the FE nor six modes reduced order model presented in Refs. [13,14] could capture dynamic pull-in instability for shock amplitudes higher than 2400g.

Recently, variety of experiments showed that the material mechanical behavior in small scales is size-dependent [15–18]. Size-dependent behavior is an intrinsic property of certain materials, which emerges when the characteristic size, e.g. the diameter or the thickness is comparable to the material length scale parameter. Material length scale parameter for a specific material can be determined using some typical experiments such as micro-torsion test [15], micro-bend test [16,17] and micro/nano indentation test [18–20]. For example, the length scale parameter for single crystals of Al, Ag, Ni, polycrystalline Cu and ploy-synthetically twinned (PST) lamellar $\alpha_2 - \mathrm{TiAl}$ and $\gamma - \mathrm{TiAl}$ have been determined, respectively, as: 2762 nm, 6233 nm, 4315 nm, 1120 nm, 74 nm and 49 nm [21].

The classical continuum mechanics cannot predict the size-dependent behavior of materials which occurs in micron and sub-micron scale structures. To remove this incapability of the classical continuum mechanics, the size-dependent continuum theories have been developed [15,22–27]. These theories contain some additional material constants besides two classical Lame's constants for isotropic materials: The classical couple stress (CCST), the classical strain gradient (CSGT), the modified couple stress (MCST) and the strain gradient (SGT) theories of elasticity include two, five, one and three additional material constants, respectively [15,23,26,27]. The size-dependent behavior of mechanical structures at micron and sub-micron scales motivated many researchers to develop some mechanical models using these size-dependent theories. Kong et al. [28] as well as Kahrobaiyan et al. [29] developed linear and non-linear Euler–Bernoulli beam formulations based on the SGT, respectively. Akgöz and Civalek [30] presented a bending analysis for uniformly loaded Euler–Bernoulli micro-beams on the basis of SGT. They also investigated the size-dependent buckling of axially loaded micro-scale beams and tubules using this theory [31,32]. Also, Ghayesh et al. [33] investigated non-linear forced vibration of a micro-beam under harmonic excitation using the SGT.

In view of the difficulties involved in determining higher-order material constants [27,34] and the approximate nature of beam theories, the MCST of elasticity has been elaborated by Yang et al. [26] which has very desirable features such as including only one additional material length scale parameter and using a symmetric couple stress tensor.

Recently, the MCST has been successfully utilized to predict mechanical behavior of micro-beams. Here some of these works are reviewed. Park and Gao [35] showed that the bending rigidity predicted by the MCST is larger than that calculated by the classical theory (CT) and the difference between the deflections predicted by these two models is significant when the beam thickness is small. Kong et al. [36] investigated the size effect on natural frequency of the Euler–Bernoulli micro-beam.

Ma et al. [37] developed a size-dependent Timoshenko beam model based on the MCST and solved the static bending and free vibration problems of a simply supported micro-beam. They showed that both the deflection and rotation of the size-dependent model are smaller than those predicted by the classical based Timoshenko beam model. Furthermore, the natural frequency predicted by the MCST is larger than that obtained by the CT. Ke et al. [38] studied the thermal effect on the free vibration and buckling of micro-beams using the MCST and Timoshenko beam theory through the differential quadrature method (DQM). Ke and Wang [39] also investigated dynamic buckling instability of functionally graded (FG) micro-beams utilizing the MCST and Timoshenko beam model. Ke et al. [40] also investigated non-linear free vibration of FG Timoshenko micro-beam using the MCST and solved the resulting equations through iterative DQM. Kahrobaiyan et al. [41] investigate the size effect on the resonant frequency and sensitivity of atomic force microscope (AFM) micro-cantilevers. Based on their numerical results, when the ratio of beam thickness to the material length scale parameter is less than 10, the difference between the results of MCST and CT is considerable for both resonance frequencies and sensitivities. Rahaeifard et al. [42] investigated the size effect on the deflection and static pull-in voltage using the MCST. They could remove the gap between the experimental observations and the results of CT for the static pull-in voltage and calculated the silicon length scale parameter as $l = 0.592\ \mu m$. Kong [43] introduced an analytic approximate solution to static pull-in problem and calculated pull-in voltage and pull-in displacement based on the MCST using the Rayleigh–Ritz method. He found that pull-in voltage predicted by the MCST is 3.1 times greater than that predicted by the CT when the micro-beam thickness is equal to material length scale parameter. Furthermore, the normalized pull-in displacement is size-independent and equals to 0.448 and o.398 for cantilever and clamped–clamped micro-beams, respectively.

Although many researchers have dealt with the mechanical behavior of micro-beams, the research effort devoted to dynamic pull-in analysis of electrostatically actuated micro-beams are very limited. The objective of present work is to establish a dynamic pull-in instability model for micro-beams under combined electrostatic actuation and shock pulse acceleration on the basis of MCST.

The present model is non-linear due to the inherent non-linearity of electrostatic excitation and geometric non-linearity of the von Kármán midplane stretching. In this study, Hamilton's principle plays a crucial rule in deriving the equation of motion. A single mode Galerkin based reduced order modeling is used to convert the partial differential equation of motion to an ordinary differential equation in time which is solved numerically using the fourth order Runge–Kutta method. It is noted that in previous studies [13,14], the shock problem was solved using multi-mode approximations in the Galerkin method. This approach for dynamic pull-in analysis is computationally expensive, so in present study an alternative simple and computationally efficient single mode approximation is utilized to solve the problem. The model predictions for both maximum amplitude of micro-beam vibration and dynamic pull-in voltage are validated through direct comparison with those calculated based on the CT in the literature. It is found that the present SDOF model can capture dynamic pull-in instability for systems under high-*g* shock accelerations. Furthermore, our model can predict dynamic pull-in voltage closer to available FE model than previous multi-mode approximations. A parametric study is also conducted to show the significant effect of couple stress components on dynamic pull-in voltage. The results show that consideration of the couple stress components in micro-system modeling is very essential especially for micro-beams in which the material length scale parameter is close to the beam thickness.

2. The modified couple stress theory

According to the MCST presented by Yang et al. [26] in 2002, both strain tensor (conjugated with stress tensor) and curvature tensor (conjugated with couple stress tensor) are included in the strain energy density. Based on this theory, the strain energy U in a deformed isotropic linear elastic material occupying region Π is given by

$$U = \frac{1}{2}\int_{\Pi}(\overleftrightarrow{\boldsymbol{\sigma}} : \overleftrightarrow{\boldsymbol{\varepsilon}} + \overleftrightarrow{\mathbf{m}} : \overleftrightarrow{\boldsymbol{\chi}})\mathrm{d}\Pi, \tag{1}$$

where $\overleftrightarrow{\boldsymbol{\sigma}}, \overleftrightarrow{\boldsymbol{\varepsilon}}, \overleftrightarrow{\mathbf{m}}$ and $\overleftrightarrow{\boldsymbol{\chi}}$ are the Cauchy stress, strain, deviatoric part of couple stress and symmetric curvature tensors, respectively. These tensors can be written as

$$\overleftrightarrow{\boldsymbol{\sigma}} = \lambda \mathrm{tr}(\overleftrightarrow{\boldsymbol{\varepsilon}})\overleftrightarrow{\mathbf{I}} + 2\mu\overleftrightarrow{\boldsymbol{\varepsilon}}, \tag{2}$$

$$\overleftrightarrow{\boldsymbol{\varepsilon}} = \frac{1}{2}\left[\nabla\mathbf{u} + (\nabla\mathbf{u})^{\mathrm{T}}\right], \tag{3}$$

$$\overleftrightarrow{\mathbf{m}} = 2l^2\mu\overleftrightarrow{\boldsymbol{\chi}}, \tag{4}$$

$$\overleftrightarrow{\boldsymbol{\chi}} = \frac{1}{2}\left[\nabla\boldsymbol{\theta} + (\nabla\boldsymbol{\theta})^{\mathrm{T}}\right], \tag{5}$$

where $\nabla = \mathbf{e}_x\frac{\partial}{\partial x} + \mathbf{e}_y\frac{\partial}{\partial y} + \mathbf{e}_z\frac{\partial}{\partial z}$, $\mathbf{u}$ is the displacement vector, λ and μ are Lame's constants (μ is also known as shear modulus), l is a material length scale parameter, $\overleftrightarrow{\mathbf{I}}$ is identity tensor and $\boldsymbol{\theta}$ is the rotation vector expressed as

$$\boldsymbol{\theta} = \frac{1}{2}\operatorname{curl}\mathbf{u}. \tag{6}$$

Obviously, only one length scale parameter l involved in addition to two Lame's constants in the constitutive equation of the MCST. The material length scale parameter l is also mathematically defined as the square of the ratio of the curvature modulus to the shear modulus and physically, is treated as a material property characterizing the effect of couple stress [37]. It is noted that both $\overleftrightarrow{\boldsymbol{\sigma}}$ and $\overleftrightarrow{\mathbf{m}}$, as respectively defined in Eqs. (2) and (4) are symmetric due to the symmetry of $\overleftrightarrow{\boldsymbol{\varepsilon}}$ and $\overleftrightarrow{\boldsymbol{\chi}}$ given in Eqs. (3) and (5), respectively.

3. MCST formulation for geometrically non-linear Euler–Bernoulli micro-beam

Fig 1 shows a schematic of clamped–clamped electrically actuated micro-beam under combined action of electrostatic and mechanical shock force. The length, width and density of micro-beam are L, b and ρ, respectively. The initial gap between the non-actuated beam and the stationary electrode is d. Also, x, y and z are the coordinates along the length, width and thickness, respectively, w is deflection of the beam and t is time.

The electrostatic excitation by polarized DC voltage V without the effect of fringing field per unit length of the beam can be expressed as [44]:

$$F_{es} = \frac{\varepsilon b V^2}{2(d-w)^2}, \tag{7}$$

where ε is the dielectric constant of medium. It is noted that the fringing field does not have a sizable effect especially for the case of wide micro-beams [45].

As depicted in Fig. 1, the micro-beam is subjected to the mechanical shock force. This force is induced by an idealized impact acceleration pulse of a half-sine waveform according to JEDEC (Joint Electron Devices Engineering Council) regulations [7,8]. The shock force is transmitted to the micro-structure through its supports. According to the support excitation scheme [46], this base excitation is equivalent to apply the shock acceleration as a distributed force over the micro-structure. A shock force pulse per unit length of the micro-beam F_{sh}, can be defined as $F_{\mathrm{sh}} = F_0 g(t)$. The shock force amplitude is

$$F_0 = \rho b h a_0, \tag{8}$$

where a_0 is the amplitude of shock acceleration pulse. The half-sine shock profile can be expressed mathematically as

$$g(t) = \sin\left(\frac{\pi t}{T}\right)\underline{U}(t) + \sin\left(\frac{\pi}{T}(t-T)\right)\underline{U}(t-T), \tag{9}$$

where T is the shock duration and $\underline{U}(t)$ is the unit step function.

Due to the mismatch of both thermal expansion coefficient and crystal lattice period between substrate and micro-beam film which is unavoidable in surface micro-machining techniques, a resultant axial force F_r is applied to the micro-beam [47] as

$$F_r = \sigma_r b h, \tag{10}$$

where σ_r represents the axial residual stress.

According to the basic hypothesis of the Euler–Bernoulli beams, the displacement field $(\tilde{u}, \tilde{w})$ of an arbitrary point on the micro-beam can be expressed as [48]

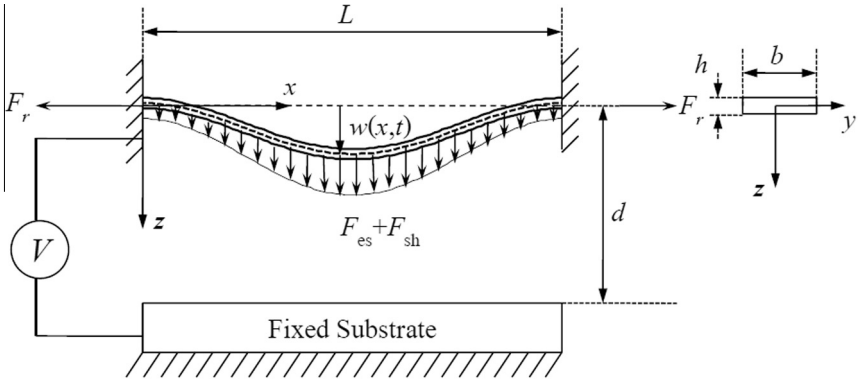

Fig. 1. Schematic of an electrically actuated micro-beam under the effect of mechanical shock.

$$\tilde{u} = u(x,t) - z\frac{\partial \tilde{w}}{\partial x}, \quad \tilde{w} = w(x,t), \tag{11}$$

where (u,w) are the axial and transverse displacement of a point on the mid-plane of micro-beam (i.e. $z = 0$). For micro-beam with small slopes after deformation, the strain components associated with the displacement field presented in Eq. (11), can be approximated by the von Kármán-type non-linear strain as [48]

$$\varepsilon_x = \frac{\partial u}{\partial x} - z\frac{\partial^2 w}{\partial x^2} + \frac{1}{2}\left(\frac{\partial w}{\partial x}\right)^2, \quad \varepsilon_y = \varepsilon_z = \varepsilon_{xy} = \varepsilon_{xz} = \varepsilon_{yz} = 0. \tag{12}$$

Hereafter, Eq. (12) will be used instead of the infinitesimal definition presented in Eq. (3). Substitution of Eq. (11) into Eq. (6) and the subsequent result into Eq. (5) yields

$$\chi_{xy} = -\frac{1}{2}\frac{\partial^2 w}{\partial x^2}, \quad \chi_x = \chi_y = \chi_z = \chi_{xz} = \chi_{yz} = 0. \tag{13}$$

For slender beam, the Poisson's effect is negligible [49], so by substituting Eqs. (12) and (13) into Eqs. (2) and (4), respectively, the non-zero components of the Cauchy stress and high-order couple stress can be determined as

$$\sigma_x = E\left[\frac{\partial u}{\partial x} - z\frac{\partial^2 w}{\partial x^2} + \frac{1}{2}\left(\frac{\partial w}{\partial x}\right)^2\right], \tag{14}$$

$$m_{xy} = -\mu l^2 \frac{\partial^2 w}{\partial x^2}, \tag{15}$$

where E is the Young modulus of the micro-beam. Upon substitution of Eqs. (12)–(15) into Eq. (1), the following result is obtained

$$U = \frac{1}{2}\int_0^L \left\{ EA\left[\frac{\partial u}{\partial x} + \frac{1}{2}\left(\frac{\partial w}{\partial x}\right)^2\right]^2 + (EI + \mu A l^2)\left(\frac{\partial^2 w}{\partial x^2}\right)^2 \right\} dx, \tag{16}$$

where I is the moment of inertia of the cross-sectional area about the y axis and A is the cross-sectional area of the micro-beam.

The virtual work done by transverse loading is

$$\delta W_{\text{trans}} = \int_0^L (F_{\text{es}} + F_{\text{sh}})\,\delta w dx = \int_0^L \left(\frac{\varepsilon b V^2}{2(d-w)^2} + F_0 g(t)\right)\delta w dx \tag{17}$$

and the virtual work done by axial residual force is

$$\delta W_{\text{axial}} = \int_0^L F_r \delta u\, dx. \tag{18}$$

The kinetic energy of the slender micro-beam with symmetric cross-section can be expressed as

$$KE = \frac{1}{2}\rho A \int_0^L \left[\left(\frac{\partial u}{\partial t}\right)^2 + \left(\frac{\partial w}{\partial t}\right)^2\right] dx. \tag{19}$$

The Hamilton principle for an elastic body is [50]

$$\int_{t_i}^{t_f} (\delta KE - \delta U + \delta W_{\text{trans}} + \delta W_{\text{axial}})\, dt = 0. \tag{20}$$

By substitution of Eqs. (16)–(19) into Eq. (20), the non-linear equations of motion are obtained as

$$\rho A\frac{\partial^2 u}{\partial t^2} - \frac{\partial}{\partial x}\left\{ EA\left[\frac{\partial u}{\partial x} + \frac{1}{2}\left(\frac{\partial w}{\partial x}\right)^2\right]\right\} = F_r, \tag{21}$$

$$\rho A\frac{\partial^2 w}{\partial t^2} - \frac{\partial}{\partial x}\left[EA\left[\frac{\partial u}{\partial x} + \frac{1}{2}\left(\frac{\partial w}{\partial x}\right)^2\right]\frac{\partial w}{\partial x}\right] + \frac{\partial^2}{\partial x^2}\left[(EI + \mu A l^2)\left(\frac{\partial^2 w}{\partial x^2}\right)\right] = \frac{\varepsilon b V^2}{2(d-w)^2} + F_0 g(t) \tag{22}$$

and the equations of corresponding boundary conditions can also be determined as

$$EA\left[\frac{\partial u}{\partial x} + \frac{1}{2}\left(\frac{\partial w}{\partial x}\right)^2\right]\delta u\Big|_{x=0}^{x=L} = 0, \tag{23}$$

$$\left\{\frac{\partial}{\partial x}\left[(EI+\mu AI^2)\left(\frac{\partial^2 w}{\partial x^2}\right)\right]-EA\frac{\partial w}{\partial x}\left[\frac{\partial u}{\partial x}+\frac{1}{2}\left(\frac{\partial w}{\partial x}\right)^2\right]\right\}\delta w\Big|_{x=0}^{x=L}=0, \tag{24}$$

$$EI\left(\frac{\partial^2 w}{\partial x^2}\right)\delta\left(\frac{\partial w}{\partial x}\right)\Big|_{x=0}^{x=L}=0. \tag{25}$$

Using Eqs. (23)–(25), the corresponding boundary conditions for clamped–clamped micro-beam are obtained as

$$u(0,t)=0,\quad EA\left[\frac{\partial u}{\partial x}+\frac{1}{2}\left(\frac{\partial w}{\partial x}\right)^2\right]_{x=L,t}=0, \tag{26}$$

$$w(0,t)=0,\quad w(L,t)=0, \tag{27}$$

$$\frac{\partial w}{\partial x}\Big|_{x=0,t}=0,\quad \frac{\partial w}{\partial x}\Big|_{x=L,t}=0. \tag{28}$$

The MEMS micro-beams are usually slender ($L/h>10$), so the longitudinal oscillation in comparison to the transverse vibration is quite small and negligible [51]. Hence, the inertia term $\rho A\frac{\partial^2 u}{\partial t^2}$ in Eq. (21) can be neglected. By setting $\rho A\frac{\partial^2 u}{\partial t^2}=0$ in Eq. (21), this equation can be solved analytically for micro-beams with constant tensile rigidity (i.e. $EA\equiv$ const.). By imposing the boundary conditions given in Eq. (26), one can obtain

$$u=-\frac{1}{2}\int_0^x\left(\frac{\partial w}{\partial x}\right)^2 dx+\left(\frac{F_r}{EA}+\frac{1}{2L}\int_0^L\left(\frac{\partial w}{\partial x}\right)^2 dx\right)x. \tag{29}$$

By substitution of Eq. (29) into Eq. (22), the governing equation of motion can be reduced to

$$\rho A\frac{\partial^2 w}{\partial t^2}+(EI+\mu AI^2)\frac{\partial^4 w}{\partial x^4}=\frac{\partial^2 w}{\partial x^2}\left[F_r+\frac{EA}{2L}\int_0^L\left(\frac{\partial w}{\partial x}\right)^2 dx\right]+\frac{\varepsilon bV^2}{2(d-w)^2}+F_0 g(t). \tag{30}$$

The initial conditions are assumed as

$$w(x,0)=0,\quad \frac{\partial w(x,0)}{\partial t}=0. \tag{31}$$

For convenience, the following dimensionless variables are introduced

$$\hat{w}=\frac{w}{d},\quad \hat{x}=\frac{x}{L};\quad \hat{t}=\frac{t}{\tilde{t}}, \tag{32}$$

where

$$\tilde{t}=\sqrt{\frac{\rho bhL^4}{EI}}. \tag{33}$$

Upon substitution of the dimensionless quantities given in Eq. (32) into Eq. (30) and *dropping the hats*, the following result will be obtained

$$(1+\alpha_1)w''''+\ddot{w}=\left[\alpha_2\int_0^1 w'^2 dx+N\right]w''+\frac{\beta}{(1-w)^2}+\alpha_3\bar{g}(t), \tag{34}$$

where dot and prime signs denote derivatives with respect to t and x, respectively. The non-dimensional parameters of the system for rectangular cross section are introduced as

$$\alpha_1=\frac{12\mu}{E(h/l)^2},\quad \alpha_2=6\left(\frac{d}{h}\right)^2,\quad \alpha_3=\frac{12\rho a_0 L^4}{Edh^2},\quad N=\frac{12F_r L^2}{Ebh^3},\quad \beta=\frac{6\varepsilon V^2 L^4}{Eh^3 d^3}. \tag{35}$$

The non-dimensional shock profile is also obtained as

$$\bar{g}(t)=\sin\left(\frac{\pi t}{T_{\text{non}}}\right)\underline{U}(t)+\sin\left(\frac{\pi}{T_{\text{non}}}(t-T_{\text{non}})\right)\underline{U}(t-T_{\text{non}}). \tag{36}$$

It is noted that, t in Eqs. (34) and (36) is non-dimensional time and T_{non} is non-dimensional shock duration expressed by

$$T_{\text{non}}=\frac{T}{\tilde{t}}. \tag{37}$$

The non-dimensional boundary conditions are

$$w(0,t) = w'(0,t) = w(1,t) = w'(1,t) = 0 \tag{38}$$

and the non-dimensional initial conditions are assumed as

$$w(x,0) = \dot{w}(x,0) = 0. \tag{39}$$

In this paper α_1, α_2, α_3, N and β are non-dimensional parameters of the system and called couple stress, gap, shock amplitude, axial force and electrostatic parameters.

4. Solution procedure

Due to the high non-linearity involved in Eq. (34), a closed-form solution for this equation cannot be found. Hence, an approximate solution based on the Galerkin weighted residual method [50] will be developed. To this end, the deflection is expressed as

$$w(x,t) = \sum_{i=1}^{M} \varphi_i(x) u_i(t), \tag{40}$$

where $u_i(t)$ is the ith generalized coordinate and $\varphi_i(x)$ is the ith non-dimensional linear un-damped mode shape of the un-deformed clamped–clamped micro-beam, normalized such that $\int_0^1 \varphi_i \varphi_j = \delta_{ij}$, where δ refers to the Kronecker delta. Since the first mode is dominant in vibration analysis [44,52], the one mode approximation has been widely used in previous studies [53–55] and proved to be very accurate for MEMS modeling. For convenience, the micro-beam deflection can be expressed as

$$w(x,t) = \psi(x)\zeta(t), \tag{41}$$

where $\zeta(t)$ is the mid-point deflection of the micro-beam and $\psi(x)$ can be determined as [56]

$$\psi(x) = \Lambda\left\{\cosh(\gamma x) - \cos(\gamma x) - \left(\frac{\cosh\gamma - \cos\gamma}{\sinh\gamma - \sin\gamma}\right)[\sinh(\gamma x) - \sin(\gamma x)]\right\}, \tag{42}$$

where

$$\Lambda = 0.6297, \quad \gamma = 4.7300. \tag{43}$$

Next, we multiply Eq. (34) by $\psi(x)$, substitute Eq. (41) into the resulting equation, integrate the outcome from $x = 0$ to 1 to obtain

$$\ddot{\zeta} + \mathrm{K}_1\zeta + \mathrm{K}_2\zeta^3 = \mathrm{K}_3\bar{g}(t) + \beta\int_0^1 \frac{\psi}{(1-\zeta\psi)^2}\,dx, \tag{44}$$

where

$$\mathrm{K}_1 = (1+\alpha_1)\int_0^1 \psi\psi''''\,dx - N\int_0^1 \psi\psi''\,dx, \quad \mathrm{K}_2 = \alpha_2\int_0^1 \psi'^2 dx, \quad \mathrm{K}_3 = \alpha_3\int_0^1 \psi\,dx. \tag{45}$$

The motion of micro-beam can be simulated by solving Eq. (44) with its zero initial conditions. Herein, this initial value problem is solved numerically using the fourth order Runge–Kutta method. It is noted that the integral $\int_0^1 \frac{\psi}{(1-\zeta\psi)^2}dx$ should be calculated numerically and repeated at the each step of integration time.

5. Results and discussions

5.1. Effect of mechanical shock on micro-structures

A micro-beam can experience the shock pulse acceleration as a quasi-static load (the response is similar to the shock profile) or as a dynamic one. Dynamic loading is experienced when the pulse duration closes to the first natural period of the micro-beam, and if the ratio of the pulse duration to the first natural period of the micro-beam is much more than the unity, the quasi-static loading will be observed. A silicon micro-beam in 110-direction with material and geometric properties listed in Table 1 is considered and no axial residual stress is assumed in this case ($N = 0$). The first natural period of this micro-beam is $\tau_1 = 0.062$ ms. It should be noted that a clamped–clamped micro-beam under sinusoidal shock profile can

Table 1
Geometric and material properties of the 110-direction silicon micro-beam.

$L(\mu m)$	$b(\mu m)$	$h(\mu m)$	$d(\mu m)$	E(GPa)	μ(GPa)	ρ(kg/m^3)	l (μm) [42]
900	100	1.5	2	169	65	2332	0.592

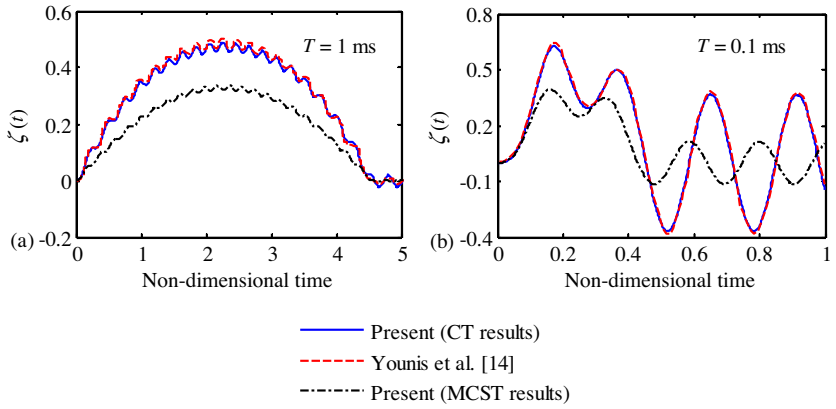

Fig. 2. Comparison between the results of present study for time history of normalized mid-point deflection of silicon micro-beam with properties presented in Table 1 and those presented by Younis et al. [14]. (a) Quasi-static loading and (b) dynamic loading case.

experience a quasi-static loading for cases with $T/\tau_1 > 4.5$ [14] and dynamic loading may be experienced in other cases. The duration of shock pulse is typically ranges from 0.2 to 1 ms for the drop table test [8], so quasi-static is more usual than dynamic loading. In this study, shock durations $T = 1$ ms and $T = 0.1$ ms will be used for simulating quasi-static and dynamic loading cases, respectively, for the silicon micro-beam with properties presented in Table 1. To validate the present analysis, the time response of both quasi-static and dynamic loading cases are compared to the results of four symmetric modes approximation presented by Younis et al. [14] for the case with no input voltage. Fig. 2(a) and (b) depict this comparison for quasi-static and dynamic loading cases, respectively. It is noted that Younis et al. [14] utilized the classical theory (CT) in their analysis, so we set $\alpha_1 = 0$ in our calculations. A very good agreement between four symmetric modes approximations and our alternative single mode solution can be observed. It should be noted that Younis et al. [14] multiply both sides of the governing equation of motion by the denominator of electrostatic forcing term, but we solved the problem without this multiplication. Hence, using the fractional term of electrostatic forcing instead of multiplication both sides of the governing equation by the denominator of this term is proposed for non-linear dynamic MEMS problems. The MCST results are also plotted in Fig. 2 to illustrate the difference between the classical continuum theory and MCST predictions. The relative difference between the CT and MCST predictions for maximum mid-point deflection, $(\zeta_{max}^{CT} - \zeta_{max}^{MCST})/\zeta_{max}^{CT}$, is 31.16% and 37.10% for quasi-static and dynamic loading cases, respectively. Hence, the size-effect is more considerable for dynamic than quasi-static loading case.

The maximum normalized amplitude of the micro-beam versus the amplitude of shock acceleration for both quasi-static and dynamic loading cases has been also plotted in Fig. 3 and compared with those obtained by Younis et al. [14] (both four modes Galerkin approximations and three-dimensional FEM predictions) as well as the MCST results. It should be noted that neglecting the effect of couple stresses may lead to very inaccurate results especially for dynamic loading case.

Fig. 4 shows both linear and non-linear ratio of the MCST to CT results for the maximum amplitude of micro-beam oscillations versus the size effect parameter h/l under two different shock acceleration amplitudes. Based on Fig. 4, neglecting the

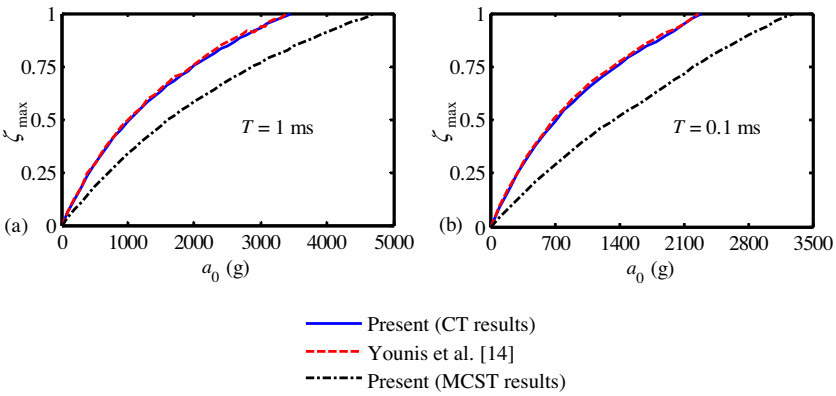

Fig. 3. Comparison between the results of present study for maximum amplitude of micro-beam vibration versus the amplitude of shock acceleration and those prepared by Younis et al. [14] (both four modes Galerkin approximations and three-dimensional FEM results). (a) Quasi-static and (b) dynamic loading case for micro-beam with properties presented in Table 1.

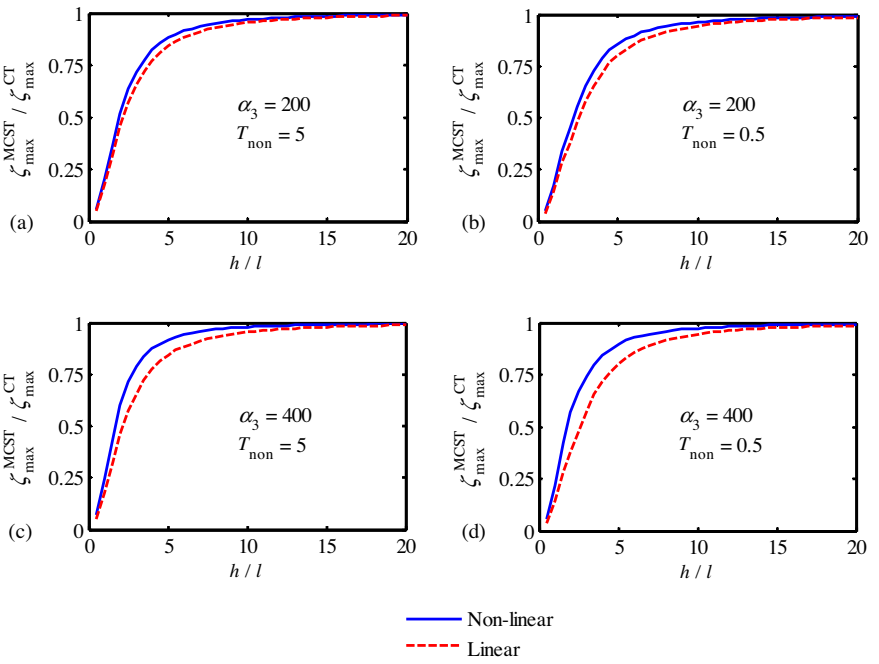

Fig. 4. Linear and non-linear ratio of maximum normalized amplitude of micro-beam oscillations calculated by the MCST to those evaluated by the CT for a micro-system with non-dimensional properties $\nu = 0.3$, $\alpha_2 = 6$, $\alpha_3 = 200, 400$ and $\beta = N = 0$ in both quasi-static ($T_{non} = 5$) and dynamic ($T_{non} = 0.5$) loading cases versus the size effect parameter h/l.

non-linear von Kármán strains may lead to under-estimation of this ratio especially for dynamic loading case. In addition, higher amplitudes of shock accelerations may cause more sizeable difference between linear and non-linear results. Hence, it is essential to account for geometric non-linearity of mid-plane stretching as well as the components of high-order couple stress for systems under high amplitudes of shock accelerations especially in dynamic loading case. It is noted that, the size effect is negligible for $h/l > 15$.

Also, Fig. 5 emphasizes on the effect of couple stresses on the variation of maximum normalized amplitude of the micro-beam oscillations (ζ_{max}) versus the non-dimensional shock amplitude (α_3) for both quasi-static and dynamic loading cases. Based on the results of this figure, decreasing the size effect parameter, reduces the maximum normalized amplitude of the micro-beam oscillations in both quasi-static and dynamic loading cases. This is due to the fact that, accounting for couple stresses increases the bending rigidity of the micro-beam which has been addressed in some previous papers for other types of loadings [35,36,42]. In MEMS applications, Rahaeifard et al. [42,57] showed that the maximum static deflection under the certain input voltage may be decreased, if the effect of couple stresses are taken into account. Furthermore, the static pull-in voltage will also be increased in this manner. It should be noted that the results of Fig. 5 also emphasizes on the fact that the size effect can usually be ignored for shock excited micro-beams with $h/l > 15$.

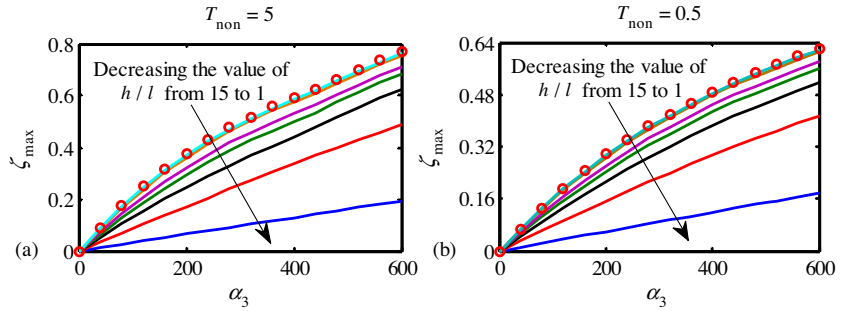

Fig. 5. Influence of the size effect parameter (h/l) on the variation of ζ_{max} versus the non-dimensional shock amplitude parameter α_3 for a micro-beam with non-dimensional properties $\nu = 0.3$, $\alpha_2 = 6$ and $\beta = N = 0$. (a) Quasi-static ($T_{non} = 5$) and (b) dynamic ($T_{non} = 0.5$) loading case. Solid lines indicate the MCST results ($h/l = 1, 2, 3, 4, 5, 10, 15$) and the markers refer to the CT predictions.

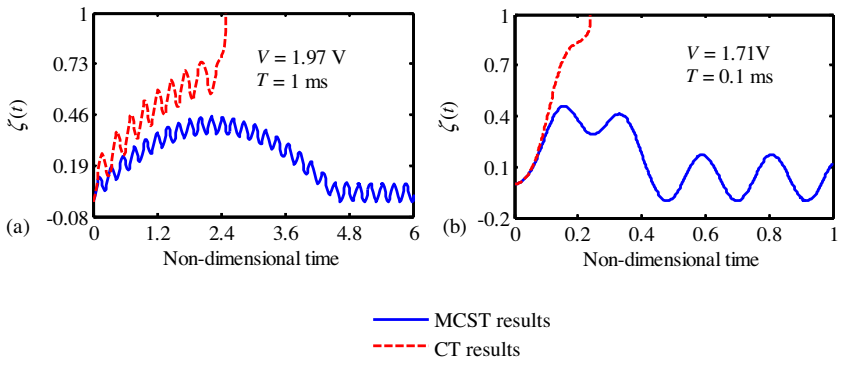

Fig. 6. Comparison between the MCST and CT results for normalized midpoint deflection of silicon micro-beam with properties presented in Table 1 (a) Quasi-static loading and (b) dynamic loading case.

5.2. The interaction between electrostatic actuation and mechanical shock

Consider the previous silicon micro-beam with material and geometric properties reported in Table 1. Dynamic pull-in voltage for this micro-beam is calculated as 3.11 V based on the CT, which agrees very well with $V_{DPI} = 3.11$ V presented by Younis et al. [14]. This voltage can be evaluated as 3.88 V on the basis of MCST. Fig. 6 depicts the mid-point deflection time history of this micro-beam under the combined effect of 1000g shock acceleration ($a_0 = 1000g$) and electrostatic actuation in both quasi-static ($T = 1$ ms) and dynamic ($T = 0.1$ ms) loading cases. It should be noted that neglecting the couple stress components may lead to under-estimation of dynamic stability threshold.

Dynamic pull-in voltages for this micro-beam versus the amplitude of shock acceleration in both quasi-static and dynamic loading cases are plotted in Fig. 7. These values are also compared and validated with the six modes approximations and FE results (the coupled electrostatic-structural element TRANS126 in commercial ANSYS software) obtained by Younis

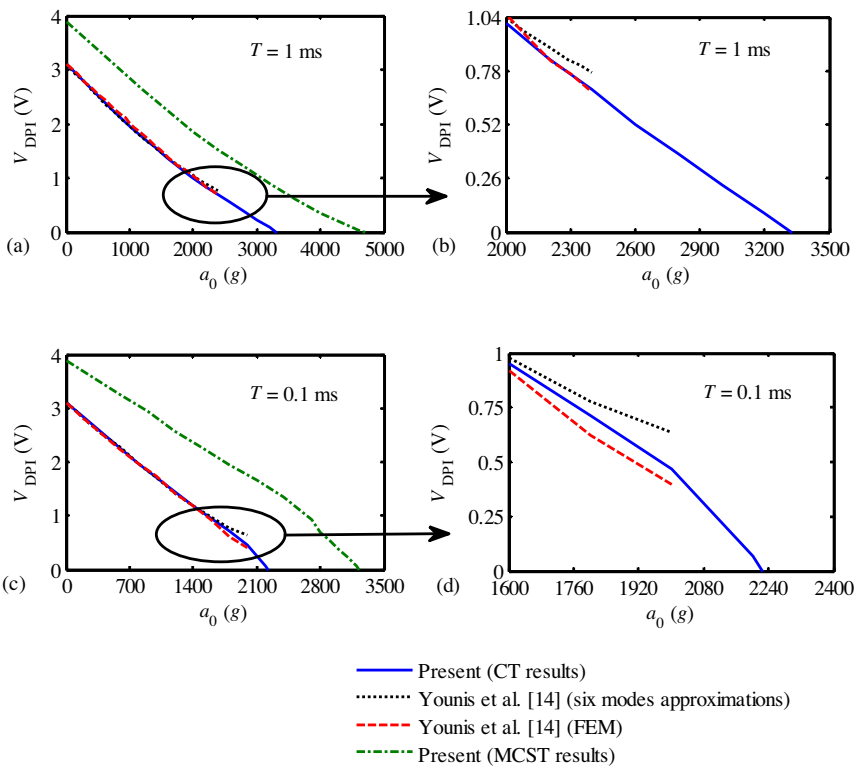

Fig. 7. Comparison between present SDOF results and those reported by Younis et al. [14] for dynamic pull-in voltage (V_{DPI}) of 110-direction silicon micro-beam with properties presented in Table 1 for both quasi-static ($T = 1$ ms) and dynamic ($T = 0.1$ ms) loading cases.

Table 2
The influence of size effect parameter on the ratio of dynamic pull-in voltages calculated by the MCST to those evaluated by the CT for a micro-system with non-dimensional properties $v = 0.3$, $\alpha_2 = 6$, $\alpha_3 = 200, 400$ and $N = 0$ in both quasi-static and dynamic loading cases.

$\frac{h}{l}$	$V_{DPI}^{MCST}/V_{DPI}^{CT}$			
	Quasi-static loading case ($T_{non} = 5$)		Dynamic loading case ($T_{non} = 0.5$)	
	$\alpha_3 = 200$	$\alpha_3 = 400$	$\alpha_3 = 200$	$\alpha_3 = 400$
0.5	6.68	14.49	7.54	34.05
1	3.36	6.75	3.80	15.72
5	1.14	1.33	1.22	2.24
10	1.04	1.08	1.06	1.33
15	1.02	1.00	1.03	1.15
20	1.00	1.00	1.00	1.08
30	1.00	1.00	1.00	1.00

et al. [14]. It can be observed from this figure that the present SDOF model can predict the dynamic stability threshold under high amplitude of shock acceleration closer to the FE results than six modes approximations presented by Younis et al. [14], especially for dynamic loading case. Furthermore, their FE model and six modes approximations cannot predict dynamic pull-in voltage for cases with $a_0 > 2400g$ for quasi-static and $a_0 > 2000g$ for dynamic loading case [14]. This is due to the fact that Younis et al. [14] pre-multiplied the equation of motion by the denominator of electrostatic forcing term which adds the effect of higher-order modes. Therefore, it is essential to account for the effects of these higher-order modes in the Galerkin procedure. It is to be noted that the present approach solves the problem without this pre-multiplication. As Fig. 7 depicts, using the present SDOF model can remove the abovementioned limitation of previous multi-mode Galerkin approximations and capture dynamic pull-in instability for every desired loading case. Hence, using present SDOF model instead of the six modes approximations presented in [14] is suggested due to its lower run time and its ability to capture the unstable mechanical behavior of micro-systems especially for cases with high amplitudes of shock accelerations. Based on the results of Fig. 7, increasing in the amplitude of shock acceleration can reduce the dynamic stability threshold. Therefore, it is very essential to account for the interaction between shock and electrostatic forces before designing MEM devices even for cases which operate within small ranges of electrostatic forces. This type of dynamic pull-in instability in high-g shock excited micro-systems has been also reported by Tanner et al. [4] as a strange mode of failure where the stationary comb fingers contact to the ground plane resulting in electrical short circuits.

The interaction between electrostatic and shock excitations in micro-switches can be utilized for sensing the level of shock acceleration [14]. This sensing method can have applications in systems which preserve the portable devices upon impact. The vehicles airbags can be considered as an example of these systems. In this sensing method the micro-switch can be tuned using applied DC voltage for a special shock acceleration level, in which the movable part of micro-switch collapses toward the substrate underneath it and sets the micro-switch in ON state. Therefore, it is very important to predict the dynamic stability threshold in these MEM devices accurately.

Table 2 represents the ratio of MCST to CT results for dynamic pull-in voltage in some different size effect parameters h/l. Based on this table, accounting for the size effect in shock modeling of MEM devices is very essential especially for systems under high amplitude of shock accelerations. In addition, the size effect is more considerable in dynamic than quasi-static loading case. It should be noted that the size effect can be usually ignored for cases with $h/l > 15$ and the ratio of $V_{DPI}^{MCST}/V_{DPI}^{CT}$ is calculated as $\left(\beta_{DPI}^{MCST}/\beta_{DPI}^{CT}\right)^{1/2}$ in Table 2.

6. Conclusions

Size-dependent dynamic pull-in analysis of clamped–clamped micro-beams is the main purpose of present paper. The mathematical model of the problem was prepared using non-linear and size-dependent Euler–Bernoulli beam theory on the basis of MCST. The non-linear governing equation of motion was derived utilizing Hamilton's principle and solved through simple and computationally efficient single mode approximation in Galerkin weighted residual method. The CT predictions of present model for dynamic pull-in voltage and maximum amplitude of micro-beam oscillations were compared with available FE and six modes reduced order model results in the literature and an excellent agreement between them was achieved. It was shown that the proposed model can predict dynamic pull-in voltage for a system under high shock accelerations better than previous six modes approximations in comparison to available FE results in the literature. In addition, our SDOF model could remove the limitation of previous models in capturing dynamic pull-in instability for systems under enormous shock accelerations. A parametric study was also conducted to illustrate the significant effect of couple stress components on micro-beam motion. Based on this parametric study, decreasing the size effect parameter (h/l) increases the bending rigidity of the micro-beam resulting in reducing the maximum normalized amplitude of micro-beam oscillations and increasing the dynamic stability threshold. Furthermore, the size effect on both dynamic pull-in voltage

and maximum amplitude of micro-beam oscillations can be usually neglected, when the beam thickness is 15 times or greater than the material length scale parameter.

References

[1] H.C. Nathanson, W.E. Newell, R.A. Wickstrom, J.R. Davis, The resonant gate transistor, IEEE T. Electron. Dev. 14 (1967) 117–133.
[2] G.I. Taylor, The coalescence of closely spaced drops when they are at different electric potentials, Proc. R. Soc. A 306 (1968) 423–434.
[3] N. Tas, T. Sonnenberg, H. Jansen, R. Legtenberg, M. Elwenspoek, Stiction in surface micromachining, J. Micromech. Microeng. 6 (1996) 385–397.
[4] D.M. Tanner, J.A. Walraven, K. Helgesen, L.W. Irwin, N.F. Smith, N. Masters, MEMS reliability in shock environments, in: Proc. of IEEE International Reliability Physics Symposium, 2000, pp. 129–138.
[5] X.W. Fang, Q.A. Huang, J.Y. Tang, Modeling of MEMS reliability in shock environments, in: Proc. of 7th International Conference on Solid-State and Integrated Circuits Technology, 2004, pp. 860–863.
[6] L. Meirovitch, Fundamentals of Vibrations, McGraw-Hill, Boston, USA, 2001.
[7] JEDEC Solid State Technology Association, JESD22-B110: Subassembly Mechanical Shock, Arlington, VA, 2001.
[8] JEDEC Solid State Technology Association, JESD22-B111: Board Level Drop Test Method of Components for Handheld Electronics Products, Arlington, VA, 2003.
[9] A. Béliveau, G.T. Spencer, K.A. Thomas, S.L. Roberson, Evaluation of MEMS capacitive accelerometers, IEEE Des. Test Comput. 16 (1999) 48–56.
[10] T.G. Brown, B. Davis, D. Hepner, J. Faust, C. Myers, P. Muller, T. Harkins, M. Hollis, C. Miller, B. Placzankis, Strapdown microelectromechanical (MEMS) sensors for high-G munition applications, IEEE Trans. Magn. 37 (2001) 336–342.
[11] M.S. Fan, H.C. Shaw, Dynamic response assessment for the MEMS accelerometer under severe shock loads, in: Proc. of NASA, 2001, TP-2001-20997.
[12] G.X. Li, J.R. Shemansky, Drop test and analysis on micro-machined structures, Sensor. Actuators A 85 (2000) 280–286.
[13] M.I. Younis, R. Miles, D. Jordy, Investigation of the response of microstructures under the combined effect of mechanical shock and electrostatic forces, J. Micromech. Microeng. 16 (2006) 2463–2474.
[14] M.I. Younis, F. Alsaleem, D. Jordy, The response of clamped–clamped microbeams under mechanical shock, Int. J. Nonlinear Mech. 42 (2007) 643–657.
[15] N.A. Fleck, G.M. Muller, M.F. Ashby, J.W. Hutchinson, Strain gradient plasticity: theory and experiment, Acta Metall. Mater. 42 (1994) 475–487.
[16] J.S. Stolken, A.G. Evans, Microbend test method for measuring the plasticity length scale, Acta Mater. 46 (1998) 5109–5115.
[17] A.C.M. Chong, D.C.C. Lam, Strain gradient plasticity effect in indentation hardness of polymers, J. Mater. Res. 14 (1999) 4103–4110.
[18] A.W. McFarland, J.S. Colton, Role of material microstructure in plate stiffness with relevance to microcantilever sensors, J. Micromech. Microeng. 15 (2005) 1060–1067.
[19] M.R. Begley, J.W. Hutchinson, The mechanics of size-dependent indentation, J. Mech. Phys. Solids 46 (1998) 2049–2068.
[20] W.D. Nix, H. Gao, Indentation size effects in crystalline materials: a law for strain gradient plasticity, J. Mech. Phys. Solids 46 (1998) 411–425.
[21] M. Zhao, W.S. Slaughter, M. Li, S.X. Mao, Material-length-scale-controlled nanoindentation size effects due to strain gradient plasticity, Acta Mater. 51 (2003) 4461–4469.
[22] R.A. Toupin, Elastic materials with couple-stresses, Arch. Ration. Mech. Anal. 11 (1962) 385–414.
[23] W.T. Koiter, Couple-stresses in the theory of elasticity: I and II, in: Proc. of K. Ned. Akad. Wet. B. 67 (1964) 17–44.
[24] R.D. Mindlin, Micro-structure in linear elasticity, Arch. Ration. Mech. Anal. 16 (1964) 51–78.
[25] R.D. Mindlin, Second gradient of strain and surface-tension in linear elasticity, Int. J. Solids Struct. 1 (1965) 417–438.
[26] F. Yang, A.C.M. Chong, D.C.C. Lam, P. Tong, Couple stress based strain gradient theory for elasticity, Int. J. Solids Struct. 39 (2002) 2731–2743.
[27] D.C.C. Lam, F. Yang, A.C.M. Chong, J. Wang, P. Tong, Experiments and theory in strain gradient elasticity, J. Mech. Phys. Solids 51 (2003) 1477–1508.
[28] S. Kong, S. Zhou, Z. Nie, K. Wang, Static and dynamic analysis of micro beams based on strain gradient elasticity theory, Int. J. Eng. Sci. 47 (2009) 487–498.
[29] M.H. Kahrobaiyan, M. Asghari, M. Rahaeifard, M.T. Ahmadian, A nonlinear strain gradient beam formulation, Int. J. Eng. Sci. 49 (2011) 1256–1267.
[30] B. Akgöz, Ö. Civalek, Analysis of micro-sized beams for various boundary conditions based on the strain gradient elasticity theory, Arch. Appl. Mech. 82 (2012) 423–443.
[31] B. Akgöz, Ö. Civalek, Application of strain gradient elasticity theory for buckling analysis of protein microtubules, Curr. Appl. Phys. 11 (2011) 1133–1138.
[32] B. Akgöz, Ö. Civalek, Strain gradient elasticity and modified couple stress models for buckling analysis of axially loaded micro-scaled beams, Int. J. Eng. Sci. 49 (2011) 1268–1280.
[33] M.H. Ghayesh, M. Amabili, H. Farokhi, Nonlinear forced vibrations of a microbeam based on the strain gradient elasticity theory, Int. J. Eng. Sci. 63 (2013) 52–60.
[34] J.F.C. Yang, R.S. Lakes, Experimental study of micropolar and couple stress elasticity in compact bone in bending, J. Biomech. 15 (1982) 91–98.
[35] S.K. Park, X.L. Gao, Bernoulli–Euler beam model based on a modified couple stress theory, J. Micromech. Microeng. 16 (2006) 2355–2359.
[36] S. Kong, S. Zhou, Z. Nie, K. Wang, The size-dependent natural frequency of Bernoulli–Euler micro-beams, Int. J. Eng. Sci. 46 (2008) 427–437.
[37] H.M. Ma, X.L. Gao, J.N. Reddy, A microstructure-dependent Timoshenko beam model based on a modified couple stress theory, J. Mech. Phys. Solids 56 (2008) 3379–3391.
[38] L.L. Ke, Y.S. Wang, Z.D. Wang, Thermal effect on free vibration and buckling of size-dependent microbeams, Physica E 43 (2011) 1387–1393.
[39] L.L. Ke, Y.S. Wang, Size effect on dynamic stability of functionally graded microbeams based on a modified couple stress theory, Compos. Struct. 93 (2011) 343–350.
[40] L.L. Ke, Y.S. Wang, J. Yang, S. Kitipornchai, Nonlinear free vibration of size-dependent functionally graded microbeams, Int. J. Eng. Sci. 50 (2012) 256–267.
[41] M.H. Kahrobaiyan, M. Asghari, M. Rahaeifard, M.T. Ahmadian, Investigation of the size-dependent dynamic characteristics of atomic force microscope microcantilevers based on the modified couple stress theory, Int. J. Eng. Sci. 48 (2010) 1985–1994.
[42] M. Rahaeifard, M.H. Kahrobaiyan, M. Asghari, M.T. Ahmadian, Static pull-in analysis of microcantilevers based on the modified couple stress theory, Sens. Actuators A 171 (2011) 370–374.
[43] S. Kong, Size effect on pull-in behavior of electrostatically actuated microbeams based on a modified couple stress theory, Appl. Math. Model. 37 (2013) 7481–7488.
[44] R.C. Batra, M. Porfiri, D. Spinello, Vibrations of narrow microbeams predeformed by an electric field, J. Sound Vib. 309 (2008) 600–612.
[45] P.C.P. Chao, C.W. Chiu, T.H. Liu, DC dynamic pull-in predictions for a generalized clamped–clamped microbeam based on a continuous model and bifurcation analysis, J. Micromech. Microeng. 18 (2008) 115008. p. 115014.
[46] C.-L. Yeh, Y.-S. Lai, Support excitation scheme for transient analysis of JEDEC board-level drop test, Microelectron. Reliab. 46 (2006) 626–636.
[47] J. Qian, C. Liu, D.C. Zhang, Y.P. Zhao, Residual stresses in microelectromechanical system, J. Mech. Strength 23 (2001) 393–401.
[48] J.N. Reddy, Theory and Analysis of Elastic Plates and Shells, second ed., Taylor & Francis, Philadelphia, 2007.
[49] J.N. Reddy, Microstructure-dependent couple stress theories of functionally graded beams, J. Mech. Phys. Solids 59 (2011) 2382–2399.
[50] J.N. Reddy, Energy Principles and Variational Methods in Applied Mechanics, John Wiley & Sons, New York, 2002.
[51] M.I. Younis, MEMS Linear and Nonlinear Statics and Dynamics, Springer, New York, 2011.
[52] J.F. Rhoads, S.W. Shaw, K.L. Turner, The nonlinear response of resonant microbeam systems with purely-parametric electrostatic actuation, J. Micromech. Microeng. 16 (2006) 890–899.

[53] Y. Fu, J. Zhang, L. Wan, Application of the energy balance method to a nonlinear oscillator arising in the microelectromechanical system (MEMS), Curr. Appl. Phys. 11 (2011) 482–485.
[54] Y.H. Qian, D.X. Ren, S.K. Lai, S.M. Chen, Analytical approximations to nonlinear vibration of an electrostatically actuated microbeam, Commun. Nonlinear. Sci. Numer. Simulat. 17 (2012) 1947–1955.
[55] A.R. Askari, M. Tahani, Analytical approximations to nonlinear vibration of a clamped nanobeam in presence of the casimir force, Int. J. Aerosp. Lightweight Struct. 2 (2012) 317–334.
[56] B. Balachandran, E. Magrab, Vibrations, second ed., Cengage Learning, Toronto, 2009.
[57] M. Rahaeifard, M.H. Kahrobaiyan, M.T. Ahmadian, K. Firoozbakhsh, Size-dependent pull-in phenomena in nonlinear microbridges, Int. J. Eng. Sci. 54 (2012) 306–310.